ELSEVIER

J. Construct. Steel Res. Vol. 45, No. 2, pp. 179–198, 1998

Printed in Great Britain
PII: S0143-974X(97)00062-X 0143-974X/98 $19.00 + 0.00

Elasto-Plastic Behaviour of Plates Subjected to Heat Loads

C. Guedes Soares, J. M. Gordo & A. P. Teixeira

Unit of Marine Technology and Engineering, Instituto Superior Técnico, Universidade Técnica de Lisboa, Av. Rovisco Pais, 1096 Lisboa, Portugal

(Received 9 October 1996; revised version received 4 August 1997; accepted 27 August 1997)

ABSTRACT

The collapse of steel plates subjected to thermal loads representative of fire conditions is analysed taking into account the temperature dependence of the steel properties. A brief description of the temperature dependence of steel properties is provided as well as the approach taken to account for their change during the heating process in the numerical algorithm. A series of calculations of load temperature curves is performed for plates of different aspect ratio, slenderness, initial imperfections and boundary conditions in order to established how they affect the temperature and the collapse load of the plates. It was observed that the maximum load carrying capacity of the plates is often reached at temperatures ranging from 100°C to 200°C, a situation in which the yield stress of the material has not decreased too much yet. The effect of the elastic support of the plates is important until collapse is reached, but afterwards it can be ignored. © 1998 Elsevier Science Ltd. All rights reserved

1 INTRODUCTION

Plate elements are one of the basic components of topsides of offshore platforms, while beam-columns are the components that make the framework supporting the platform topsides. Plate elements supported by the framework make the decks and ceilings. Plates are also used in the walls of the compartments, both when they are aimed at providing blast resistance or only as a barrier for the thermal load induced by fires.

In both the horizontal and vertical components the plates can be stiffened.

However, the understanding of the behaviour of the stiffened plates builds upon the knowledge of the behaviour of the unstiffened plate elements, which provide a significant strengthening effect to the associated stiffeners.

This study considers the behaviour of rectangular plate elements under thermal loads of magnitudes that can be reached during fires in offshore platforms. The increase of temperature associated with the fires will induce a tendency for the plates to expand. However, the restrictions provided by the boundaries which may be at a lower temperature induce biaxial compression on the plates. This paper will provide load shortening curves of plates subjected to the biaxial loading associated with their temperature increase, showing the effect of the different parameters that influence the plate collapse.

The behaviour of plate elements under compressive loads has been studied for many years. Earlier treatments used linear and non-linear elastic analysis. Major developments have occurred during the early 1970s with the development of numerical procedures based on finite differences and on finite elements. It then became possible to study realistic cases of elasto-plastic collapse of plates with large deflections. Several parametric studies have been performed to indicate the effect of different parameters on the collapse strength, including the initial distortions and residual stresses [1–6].

Although most of the studies dealt with uniaxial loads, some have considered the collapse resistance under biaxial loads as reviewed in Ref. [7]. However, no studies have been identified on the collapse strength of plate elements subjected to elevated temperatures.

In fact, much research has been done related to the effect of fires on the components in building structures and here the concern has been the behaviour of columns [8–10] as well as frames [11,12].

For temperatures higher than 200°C, the stress–strain characteristics of steels change by decreasing the yield stress and the modulus of elasticity. This effect combined with the increase of stresses associated with the temperature elevation leads to the collapse of plates. A review of the stress–strain properties of steels has been provided in Ref. [13] and the main recommendations were that for current steels the average curves specified in the Eurocodes [14] are the best option whenever there is no specific data for the steel under consideration.

At ambient temperature the collapse strength of plates is governed mainly by the plate slenderness, although the boundary conditions, the aspect ratio and the initial distortions are important parameters [15].

This study has determined the load-shortening behaviour of plates with different aspect ratios, slenderness and initial distortions by using a non-linear finite element code. A proportional displacement has been imposed on the edges of the plates and the corresponding edge reactions have been calculated.

The loading is a heat source that leads to a monotonically increasing tem-

perature with uniform distribution in the plate, which varies from ambient temperature to values up to 800°C. The assumption of uniform temperature in the plates results from the thermal conductivity of steel which leads to a very quick heat conduction.

2 STEEL PROPERTIES AT HIGH TEMPERATURES

For a thermal and structural analysis a knowledge of the thermal and mechanical properties of the structural material is required. Steel does not provide any significant resistance to heat transfer and, furthermore, the thermal properties of steel that are of interest do not vary significantly with temperature, as opposed to the mechanical properties.

To calculate the strength of steel structures and components under the induced fire load temperatures it is essential to have a knowledge of the stress–strain properties of steel at elevated temperatures.

Different experimental programmes have been conducted in the past, providing stress–strain curves for different kinds of steels, and a synthesis of the results together with proposals of analytical models was presented [16–18].

The data presently available about strength of steel at high temperatures are experimental results that have been used as a basis to develop design curves. Important work has been performed in Europe related to the development of design curves for steel structures under fire loads based on data from different sources. The experimental programmes conducted so far have shown that the effect of temperature on the stress–strain curves of steel is the same for all types of steel. This is very important in that only one theoretical model is enough to describe the mechanical behaviour of all steels.

In the present study the European Recommendation [14] was used. Five different curves were defined to describe the steel properties for temperatures of 0, 200, 400, 600 and 800°C, respectively, as indicated in Fig. 1. For intermediate temperatures a linear interpolation between the two nearest curves must be made.

It can be seen that at 200°C there is a decrease of the yield and ultimate stresses but the difference between the yield stress and the ultimate stress is not very large. For 400°C, the yield stress is much lower and, although the ultimate stress is very similar to that at 200°C, it is only reached at a much larger strain. For 600 and 800°C there is a very significant decrease in the ultimate stress but the difference between the yield stress and the ultimate stress is again small, i.e. the overall behaviour again becomes similar to that at 200°C.

The stress–strain curves for different temperatures of steels of different yield stress are similar to those presented in Fig. 1, only scaled by the yield stress

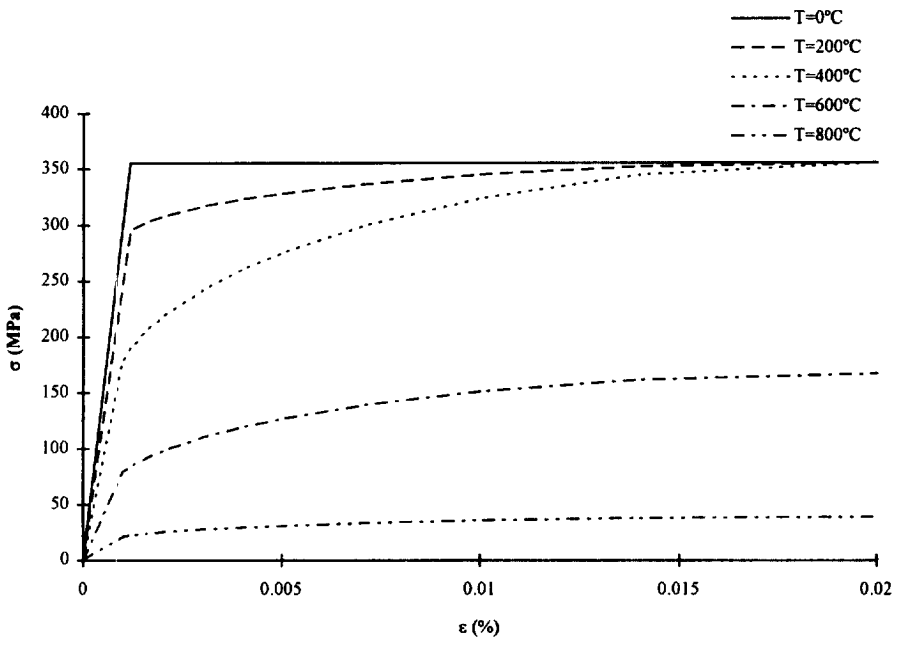

Fig. 1. Stress–strain curves for different temperatures of a high tensile steel, Fe360 [14].

at ambient temperature. The main change in the maximum stress occurs at 400°C corresponding to a sudden drop in this stress. However, for temperatures lower than that, the ratio between the proportional limit and the maximum stress increases with temperature.

Fig. 2 shows the dependence on temperature of the yield stress, maximum stress and Young's modulus, normalised by their values at ambient tempera-

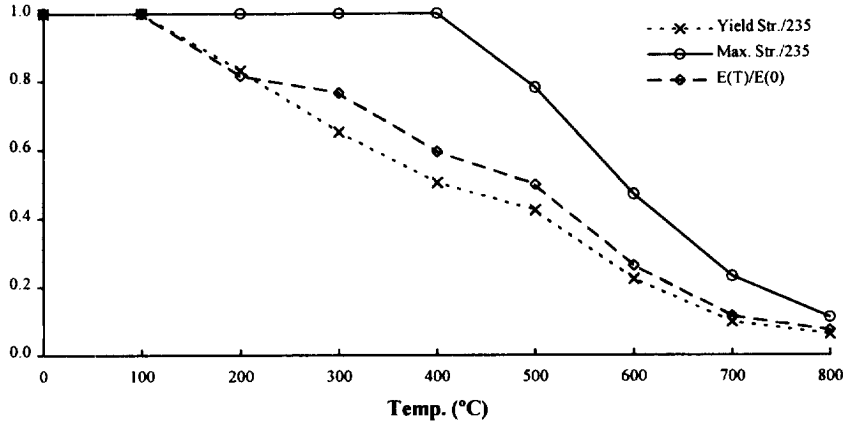

Fig. 2. Material properties of mild steel [14].

ture. It is clear that while the yield stress and the Young's modulus start to decrease at temperatures of 100°C, the maximum stress only starts to be degraded at 400°C.

3 THERMO-ELASTO-PLASTIC ANALYSIS

The numerical calculations were performed using the ASAS-NL software [19] which takes thermal loads into account. This is a general purpose non-linear finite element code in which large displacement effects are handled using an updated Lagrangian formulation with inclusion of geometric stiffness terms for plate elements.

The plasticity is modelled by the von Mises or Tresca yield criteria. The material behaviour can be non-linear and is defined by a piecewise linear, stress–strain curve for various temperatures. Properties at intermediate temperatures are obtained by linear interpolation.

The non-linear solution of a thermo-elastic-plastic analysis is approached in an incremental–iterative manner using Newton's method to solve the non-linear equilibrium equation

$$\Delta\{\delta\} = - |K_t|_i^{-1}\{\varphi\}_i \tag{1}$$

where $|K_t|_i^{-1}$ is the incremental stiffness matrix evaluated for displacement at iteration i, $\{\delta\}_i$ and the improved set of nodal displacements is given by

$$\{\delta\}_{i+1} = \{\delta\}_i + \Delta\{\delta\}. \tag{2}$$

This procedure is carried out iteratively until the unbalanced load vector $\{\varphi\}$ has converged to zero.

The incremental load vector consists of the mechanical and thermal components

$$\Delta\epsilon = \Delta\epsilon_e + \Delta\epsilon_p + \Delta\epsilon_{th} \tag{3}$$

where $\Delta\epsilon_e$, $\Delta\epsilon_p$ and $\Delta\epsilon_{th}$ are the incremental elastic, plastic and thermal strains, respectively. The temperature is increased incrementally according to what has been specified as input and the thermal load vector is computed from the thermal strain increment by

$$\Delta\epsilon_{th} = \alpha\Delta T + \Delta_\alpha T \tag{4}$$

where α is the coefficient of thermal expansion, ΔT is the temperature

increment, Δ_α is the change in α due to temperature change ΔT and T is the temperature at the beginning of the step with respect to the reference temperature state.

To compute the element stiffness the material properties are updated according to the actual thermal load. The material stiffness can either be elastic or elasto-plastic depending whether plasticity has occurred at an integration point.

After the calculation of the nodal displacements the plastic strain increment is calculated from the plastic and state information. Hence, stresses are then obtained using the constitutive law.

4 PRELIMINARY CALCULATIONS

When trying to understand the behaviour of a plate element which is part of a structure subjected to thermal loads due to a localised fire, the first problem that arises is concerned with the difference in temperature at that particular region compared with the temperature of the rest of the structure.

If one considers an unloaded structure subjected to a temperature increase, and if the whole structure has the same temperature increase, there will be no restraining boundary conditions to a substructure and thermal stresses will not be present, i.e. the whole structure will simply expand.

When there is a temperature differential within a structure, this will generate thermal stresses increasing with temperature until they reach a level that induces the collapse of the plate. After that level the plate sustains a lower level load. However, this capability is dependent not only on the temperature differential between the plate element and the rest of the structure, but may also be dependent on the 'initial temperature', i.e. the temperature of the surrounding structure.

In order to assess the effect of the initial temperature, calculations were performed for a plate of aspect ratio (a/b) equal to 1 and breadth to thickness ratio (b/t) equal to 40 and 80, which was considered for different initial temperatures ($T_i = 0$, 40, 80, 160 and 240°C). From these initial states the temperature applied to the plate was increased to 800°C, keeping the boundary conditions of the plate restrained to linear displacements in its plane.

Temperature is considered to be uniform over the whole plate, which is often the situation when it is assumed in this study that fires have much larger dimensions then the structural components.

Figs 3 and 4 show the curves obtained for the different initial temperatures of the plates with b/t ratio of 40 and 80. It is clear that the post-collapse strength is very similar, although the collapse temperature and the collapse load depend on the initial temperature of the plate. However, the collapse

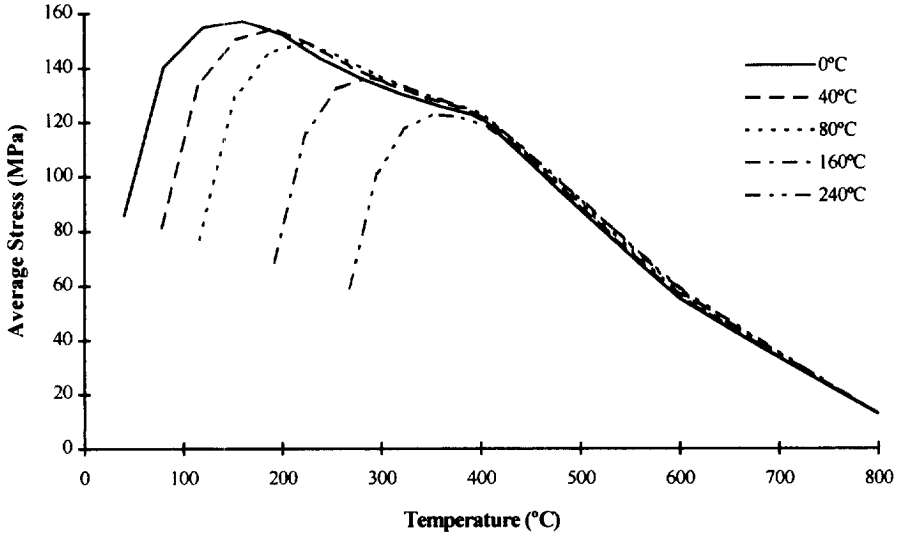

Fig. 3. Influence of the initial temperature in the curves of stress temperature differential for a square plate with $b/t = 40$.

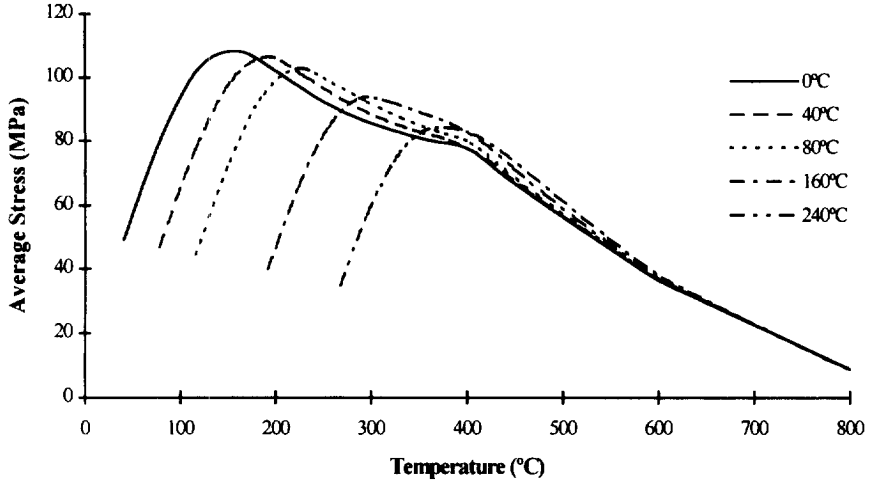

Fig. 4. Influence of the initial temperature in the curves of stress temperature differential for a square plate with $b/t = 80$.

load of plates that have a high initial temperature lies almost over the stress–temperature post-collapse curve of the plates that start from a lower temperature.

Some difference may be detected when passing from stocky to slender plates. In the latter, the collapse load for the plates that have high initial temperature is above the post-collapse curve for the plates that start from

ambient temperature, while the difference is not marked in the stocky plates. This behaviour is the consequence of the effect of load shedding after buckling which is much more important in slender plates than in stocky ones when a reasonable level of initial imperfections is considered.

The post-buckling load shedding is directly related to the increase of the deformations and to the amount and spread of plastic strain, which tends to soften the structure. In the slender plates, the effective width is only a small part of the plate width and consequently the amount of plastic strain near the edges is much greater than in the rest of the plate, contributing to the increase in out-of-plane deformations and reduction of the actual carrying capacity of the plate at that temperature. When, for similar plates, one is considering a low and a high initial temperature, the collapse temperature of the second corresponds to a lower degree of plasticity and a smaller magnification of the deformations compared with the state of the first at the same temperature, and thus its strength will be higher.

This explanation would lead one to expect that the difference between the two curves will be kept constant for temperatures higher than the collapse temperature. However, the reduction of the yield and maximum stresses of the steel due to the temperature increase will play an increasing role by adding a supplementary plastic strain that speeds up the process by magnifying the deformations to levels such that their amplitude becomes irrelevant to the plate strength.

Finally, it should be observed that the temperature difference that promotes the collapse is kept constant. Thus, in the range of analysis ($0 < T_i < 240°C$), the average strain necessary to produce the collapse of the plate may be represented approximately by the initial yield strain. This is equivalent to dealing with a temperature, since they are related by the coefficient of thermal differential expansion ($\alpha_t = 1.1 - 1.4 \times 10^{-5}/K$), which does not change with temperature.

As a first conclusion, one may say that the only consequence of the different initial temperature of the plates is the change of the collapse load of the plate, which is directly related to the reduction of the maximum and yield stresses with increasing temperatures. However, this collapse load seems to be of reduced interest in structures subjected to fire, where temperature differences larger than 120°C are normal.

5 PARAMETRIC STUDY

Having established that the thermal collapse load of plates is independent of their initial temperature, a series of calculations was conducted for several plates starting from an initial ambient temperature, subjected to a temperature

increase up to collapse and continuing in the post-collapse range. The aspect ratio of the plates is 1 and 3, and the slenderness covered ranges from b/t = 20 to 100.

The nominal plate slenderness is defined at ambient temperature as

$$\beta = \frac{b}{t}\sqrt{\frac{\sigma_0}{E}} \tag{5}$$

where σ_0 and E are the yield stress and Young's modulus, respectively. However, when dealing with changing temperature, the definition of the plate slenderness presents a difficulty since the material properties of the plate are changing with temperature. Thus it is less meaningful to identify a plate with its slenderness at ambient temperature. In order to avoid this problem the plates were identified by their b/t ratio.

The effect of initial geometric imperfections was also investigated. Considering two levels of imperfections, 'almost' perfect plates, denoted as A, were given a maximum lateral displacement of 1 mm. A plate was considered as having average distortions, and denoted as C when

$$w_{max}/t = 0.10\beta^2$$

where β is the plate slenderness at ambient temperature.

Another two levels of imperfections were investigated, but due to the reduced importance of the initial imperfections they were not considered further in the calculations.

The shape of the initial imperfections may be represented by a Fourier series as

$$w = \sum_m \sum_n \delta_{mn} \sin \frac{m\pi x}{a} \sin \frac{n\pi y}{b} \tag{6}$$

where a and b are the plate dimensions and δ_{mn} are the amplitude of the components.

In each calculation the initial distortion of the plate was represented by a shape with only one component of this series. However, each type of plate was considered twice with a different initial distortion described by the order (m, n) of the Fourier component of the initial distortions in order to quantify the sensitivity to this parameter. Thus all plates were run with the pair (m = 1; n = 1) and some of them with the pair ($m = a/b$; n = 1). The latter proved to have the same response as the square plates and thus their behaviour may be represented by the behaviour of these plates.

5.1 Restrained boundary conditions

Fig. 5 shows the load–temperature curves for plates of high strength steel (Fig. 1) with $a/b = 1$ but with different slenderness ($b/t = 20$, 40, 60, 80 and 100). Each pair of curves indicates the relationship between the stress and the temperature increase for the two levels of initial imperfections. The main conclusion that one may draw from those results is the insensitivity of the post-buckling collapse strength with respect to the initial imperfections in square plates. Furthermore the effect of imperfections on the ultimate load is negligible for plates with $b/t > 60$.

The stresses indicated in Fig. 5 may be understood as the longitudinal or the transverse stresses since they are the same for square plates due to symmetry. This means that the strength of the plates under thermal loads has to be understood as the biaxial strength instead of uniaxial strength.

For plates of $a/b = 3$ a more detailed coverage of the range of slenderness was considered. Two levels of imperfections and two shapes of distortions were considered. Fig. 6 compiles the results of 'almost' perfect plates (maximum initial imperfections of 1 mm).

The biaxial state of stresses is well present in all plates, especially in the elastic range ($T < 100°C$). Collapse in the transverse direction is reached at a lower temperature and at lower stress levels, after the collapse in the transverse direction, the stresses in this direction fall quickly to very low levels while

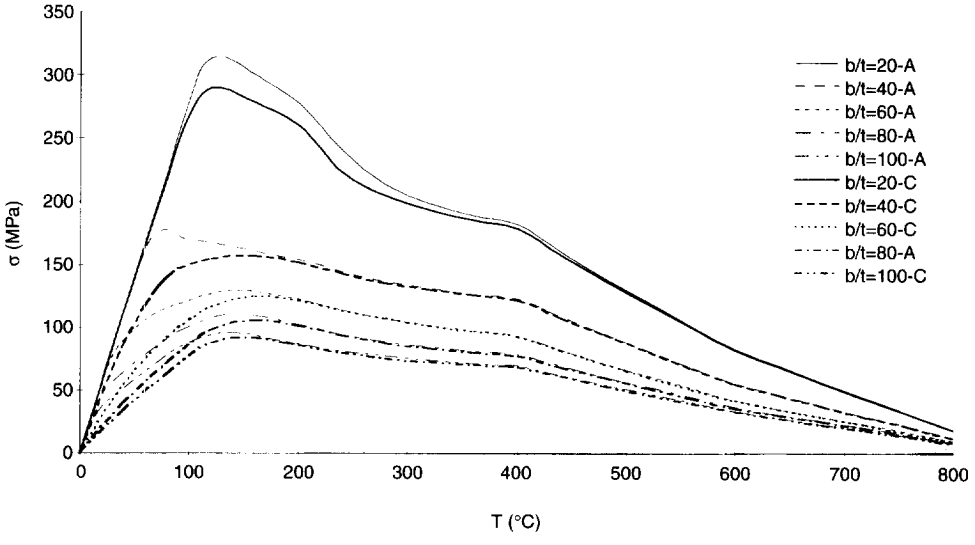

g. 5. Stress–temperature curves of square plates of high strength steel with different initial imperfections.

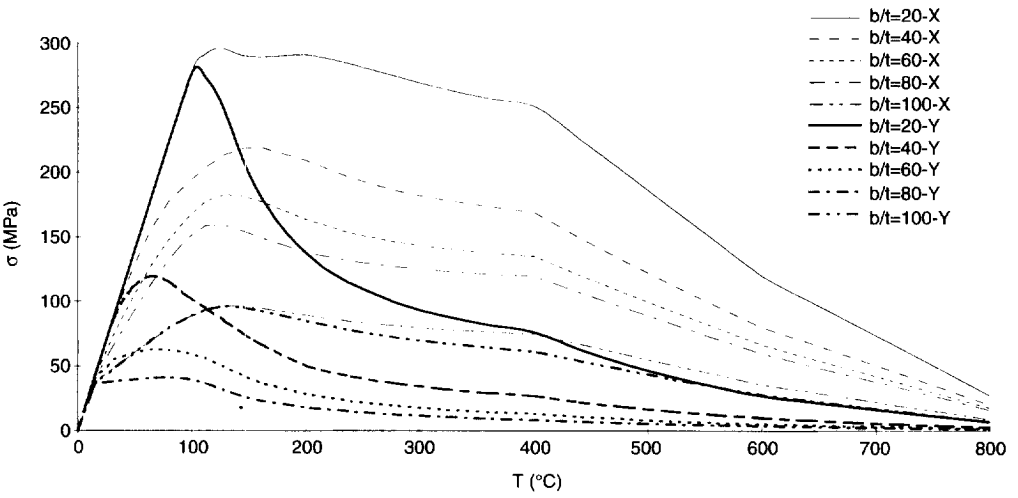

Fig. 6. Stress–temperature curves of rectangular plates ($a/b = 3$) of high strength steel with shape of imperfections of type A (almost perfect); X denotes the stresses in the longitudinal direction and Y in the transverse direction.

the longitudinal stresses keep increasing until the longitudinal collapse is achieved.

The first main conclusion for plates with aspect ratio different from that with a predominant mode of imperfections equal to the length of the plate is that the collapse in the transverse direction is achieved at lower temperatures ($T \approx 75°C$) than the collapse in the longitudinal direction or the collapse of square plates ($T \approx 120°C$) in which failure occurs simultaneously in both directions. This behaviour is confirmed when average initial imperfections are used, Fig. 7.

However, two main differences may be observed when dealing with different imperfections. First, the collapse in both directions is achieved at lower stresses with increasing imperfections, which confirms the same conclusion for square plates; second, very slender plates may exhibit a 'strange' behaviour when the distortions are very low.

In the present case, 'almost' perfect plates with $b/t = 100$ change their shape of deformation in the elastic range to a mode $m = \alpha$ which makes the collapse similar to that of a square plate. After collapse, the transverse stress tends to be lower than the longitudinal stress due to the effect of the mode of the initial imperfections, $m = 1$, which is still present. The influence of the initial imperfections is confirmed to be negligible, apart from the mentioned case of $b/t = 100$ with very low imperfections level, in which a change in the mode of collapse occurs, Fig. 8.

Fig. 9 has results of a plate of $b/t = 60$ and is a typical example of the lack

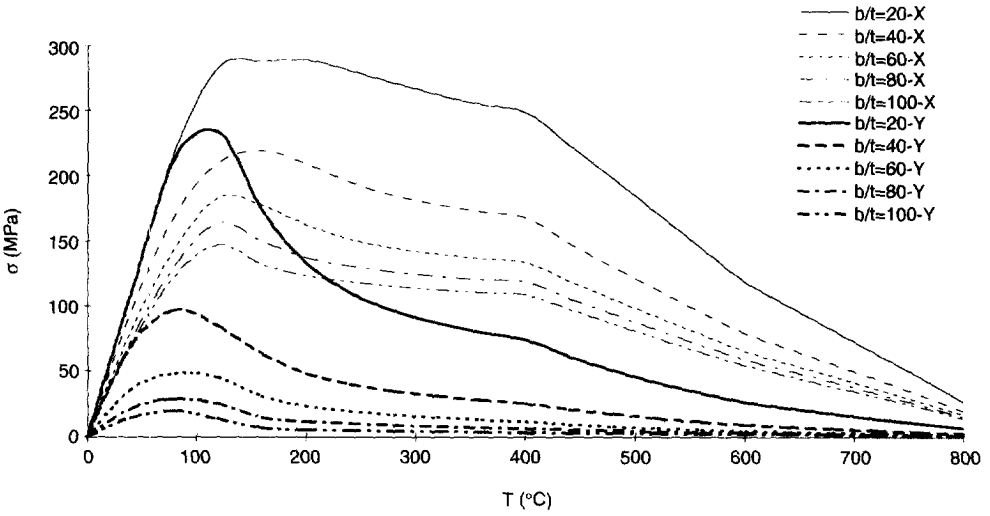

Fig. 7. Stress–temperature curves of rectangular plates (a/b = 3) of high strength steel with shape of imperfections of type C (average distortion); X denotes the stresses in the longitudinal direction and Y in the transverse direction.

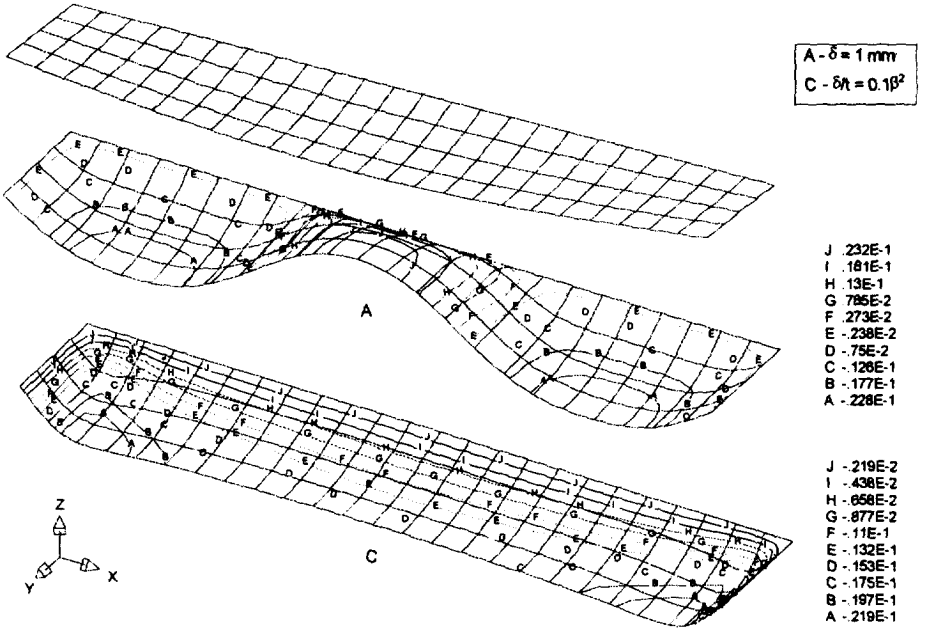

Fig. 8. Deflections of plates α = 3 and b/t = 100 for small (A) and large (C) imperfections at initial collapse, showing the different modes of collapse.

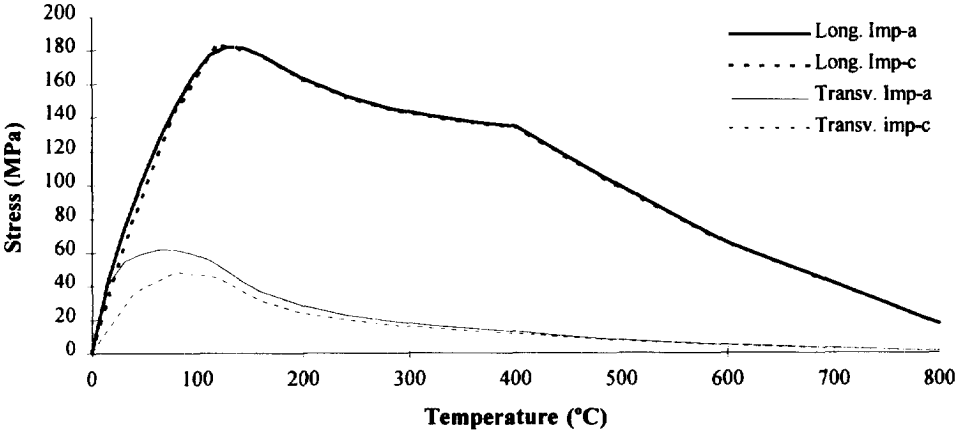

Fig. 9. Stress–temperature curves of rectangular plates (a/b = 3) of high strength steel and b/t = 60 for two levels of imperfections.

of sensitivity to the level of imperfections, when dealing with temperature load. In the elastic range some differences in the behaviour of the plate due to initial imperfections may be detected, but after collapse of the plate the curves of the stresses in each direction tend to be independent of distortions. Transverse stresses are more sensitive to imperfections because, for a plate with this aspect ratio and mode of imperfection, the first collapse is in that direction. However, far beyond the collapse, the influence of distortions tends to disappear even in the transverse direction.

A detailed analysis of Figs 5–7 shows a discontinuity of the derivative of $\sigma(T)$ at 400 and 600°C, which may be the consequence of a too crude definition of the material properties, i.e. a large step in the difference of temperature that defines the material behaviour. Because of that a second series of analysis was carried out using the properties of mild steel, and a step half of that used earlier (i.e. a step of 100°C). This analysis also allows us to study the influence of the different material properties.

Figs 10 and 11 plot the results for plates with an aspect ratio of 1 and 3. These figures shall be checked against Figs 5 and 7.

Fig. 12 illustrates the out-of-plane deflection against temperature of a square plate, showing that a large level of deflection is attained for high temperatures.

Fig. 13 compares the behaviour of the plates with average imperfections using different steps on the definition of material properties and with different yield stresses. Two main conclusions may be inferred from the analysis of the figure. First, the behaviour is only scaled by the yield stress. If the curves of material properties in the range of temperatures have the same shape for two materials with different yield stress, then the behaviour at high temperatures, i.e. in the post-collapse regime, is only scaled by the yield stress.

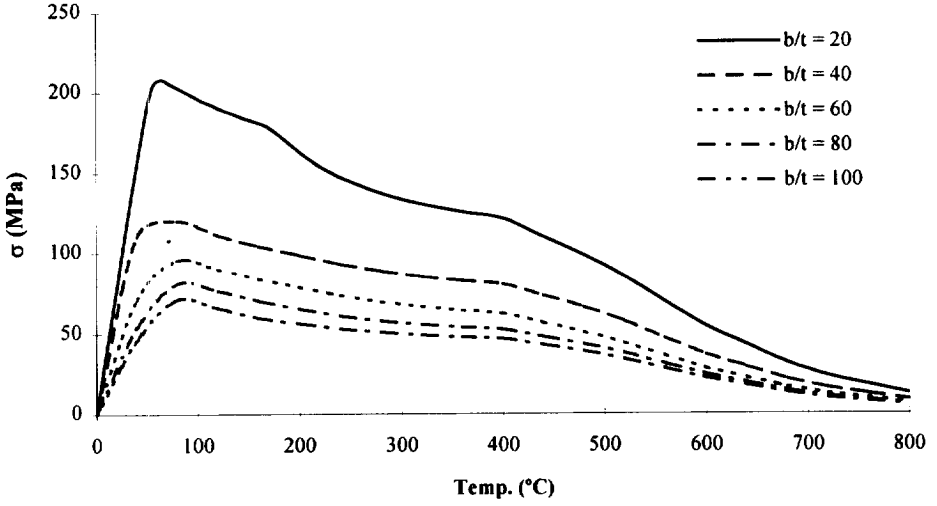

Fig. 10. Longitudinal stress–temperature curves of square plates (a/b = 1) with different slenderness for mild steel.

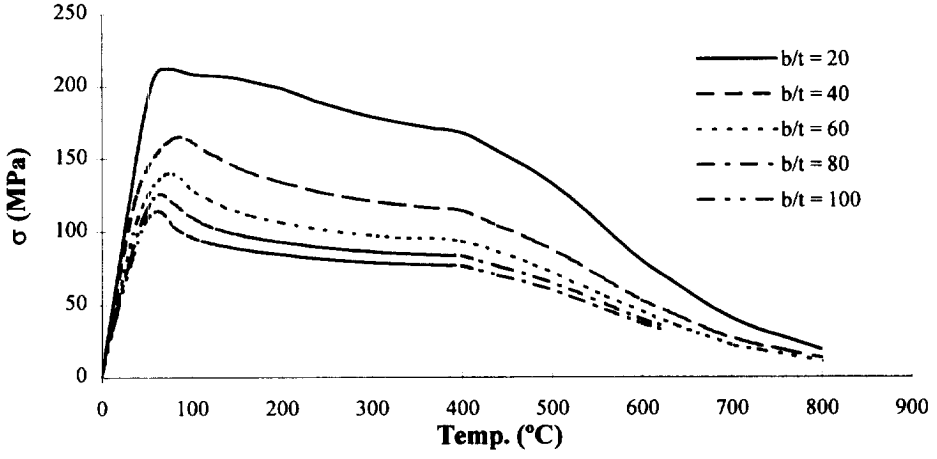

Fig. 11. Longitudinal stress–temperature curves of rectangular plates (a/b = 3) with different slenderness for mild steel.

Second, in the pre-buckling domain the average stress–temperature curves depend very much on the yield stress due to the variation of the effective plate slenderness at the loading point with the yield stress even for plates with the same b/t ratio [20].

The fact that one may associate an average strain to the temperature scale instead of an average normalised strain is the main cause of the different derivative of the curves of material with the same b/t ratio and of the different

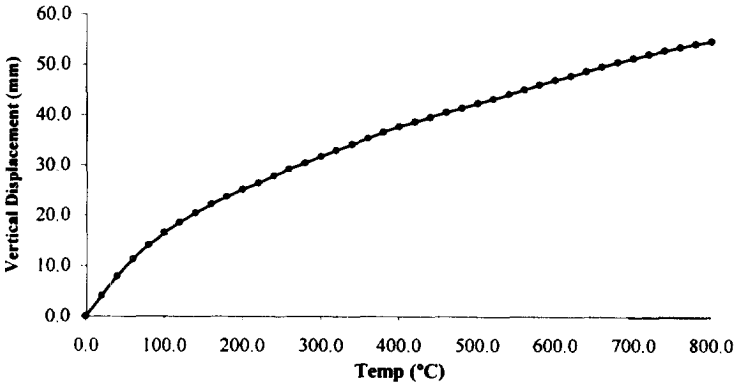

Fig. 12. Vertical displacement–temperature curve of a square plate for mild steel (a/b = 60).

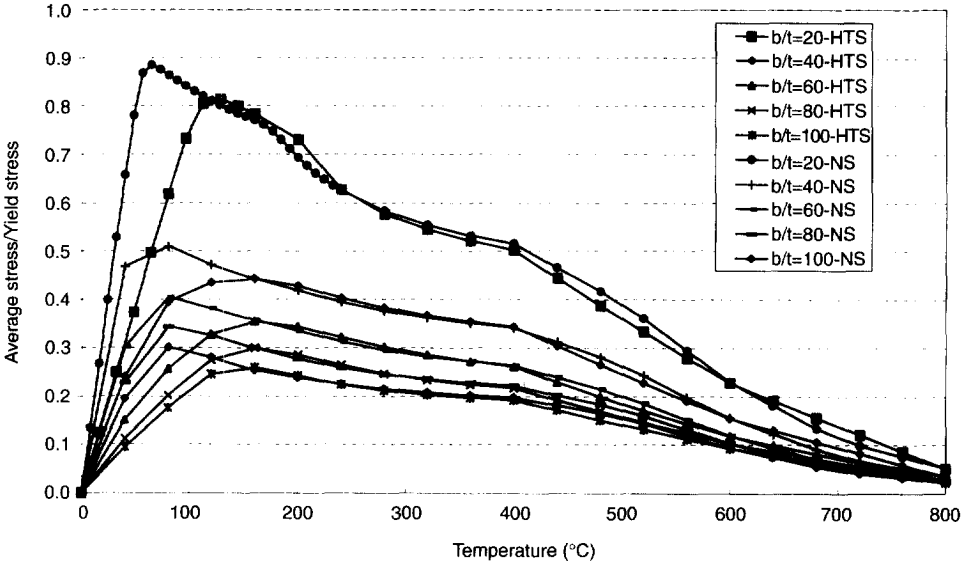

Fig. 13. Comparison of the normalised stress–temperature curves of square plates with higher strength steel (HSS) and with mild steel (NS).

temperature of collapse. The difference in the collapse load for the same b/t ratio is due to the different nominal slenderness consequence of the yield stress in the two cases, i.e. plates with a higher yield stress than those of normal steel have a higher nominal slenderness and thus a lower normalised ultimate stress, usually denoted as ultimate strength.

At the temperature of collapse of a plate of normal yield stress it has the same effective slenderness as the high tensile steel plate, thus the stress at that temperature should be similar for the two plates. The differences may be

a result of the actual state of imperfections in the two plates, but this parameter has little effect when dealing with temperature, as pointed out before.

Some differences between the curves of the same b/t ratio are observed at temperatures around 500 and 700°C, which are a direct consequence of the improvement in the resolution of the material properties with temperature for the case of normal steel, where the properties were defined at 500 and 700°C while for the HTS they were estimated by interpolation.

5.2 Elastic supports

In real structures the supports of the plate elements are the stiffeners and the surrounding structure. The former provide support mainly for out-of-plane displacements, while the latter restrain the in-plane displacements. Thus, the boundary conditions of the plate elements are far from being fixed when they are thermally loaded.

In a first approach the elastic support to in-plane displacements may be taken proportional to the area of the edge and the modulus of elasticity. This assumes that the stiffeners do not support any load in these directions and the surrounding plating has a similar thickness as the loaded plate. The constant of proportionality depends mainly on the geometry and dimensions of the frames that are oriented in the same directions of the displacements, on the ratio between the thickness of the plate and of the surrounding structure and, eventually, on the particular position of the plate on the panel.

Using these considerations, springs were connected to the nodes perpendicular to the edges with a rigidity proportional to $K_0 = EA/a$, where a is the length of the plate in a direction perpendicular to the edge and A is the cross-sectional area ($A = bt$). Two levels were used: K_0 and $0.5K_0$.

Figs 14–18 compare the stress–temperature curves varying the degree of restraint to in-plane displacements for five b/t ratios. The shape of each curve is similar to the others apart from a magnification of the scale due to the slenderness.

However, the curves of plates with $b/t = 20$ have a slight difference from the others. For other slendernesses the curves with low rigidity at the boundary always have lower strength at the same temperature as those with high rigidity. However, in stocky plates the amount of plastic strain seems to be very important at low temperatures, $T < 400$°C. A large plastic strain tends to magnify the out-of-plane imperfections and this reduces very much the strength comparative to plates where the plastic strain, and consequently the imperfections, are low.

This analysis is general but in stocky plates with average imperfections the ratio between the maximum initial distortions and the thickness is very low, thus the magnification of imperfections at buckling changes the shape of the

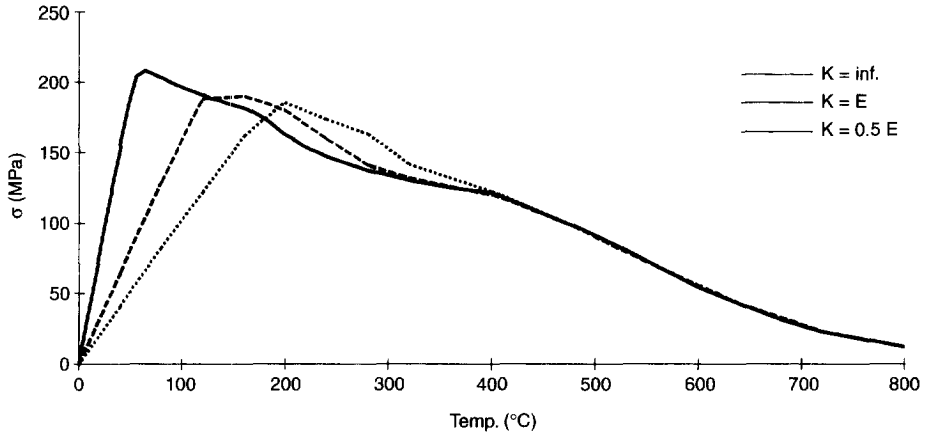

Fig. 14. Comparison of the stress–temperature curves of plates with different rigidity at the edges and $b/t = 20$, for mild steel.

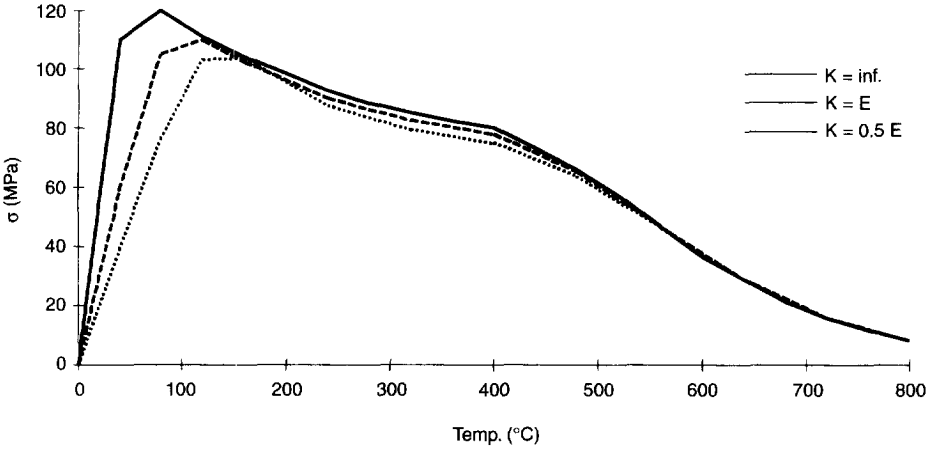

Fig. 15. Comparison of the stress–temperature curves of square plates with different rigidity at the edges and $b/t = 40$, for mild steel.

plate from an almost perfect plate before buckling to a plate with a marked mode of collapse. When comparing the plate already buckled due to high constraint with the one in a pre-buckling state due to reduced constraint, the level of imperfections at the same temperature is very different and much lower in the latter case, which makes it have a higher strength than the former plate.

The other significant consequence of reducing the rigidity at the edges is the increase of the collapse temperature from around 100°C to 180°C. This is an expected result which may be very important in the design of the structures.

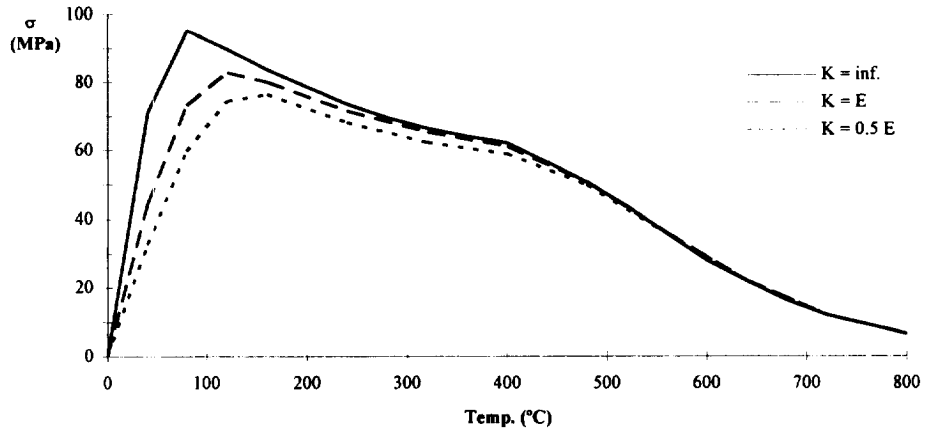

Fig. 16. Comparison of the stress–temperature curves of square plates with different rigidity at the edges and $b/t = 60$, for mild steel.

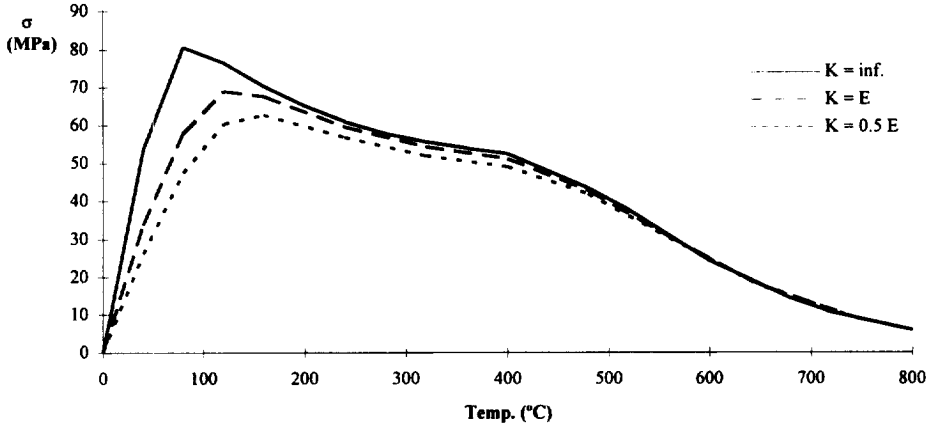

Fig. 17. Comparison of the stress–temperature curves of square plates with different rigidity at the edges and $b/t = 80$, for mild steel.

6 CONCLUSIONS

This study has provided the load–temperature curves for several plates ranging from $a/b = 1$ to $a/b = 3$ and from $b/t = 20$ to $b/t = 100$ with different levels and shapes of initial distortions.

It was observed that the maximum load carrying capacity of the plates is often reached at temperature differentials ranging from 100°C to 200°C, a region where the yield stress of the material has not decreased too much yet.

The effect of the elastic supports of the plates is important until the collapse of the plate is reached, but afterwards it may be ignored. However the

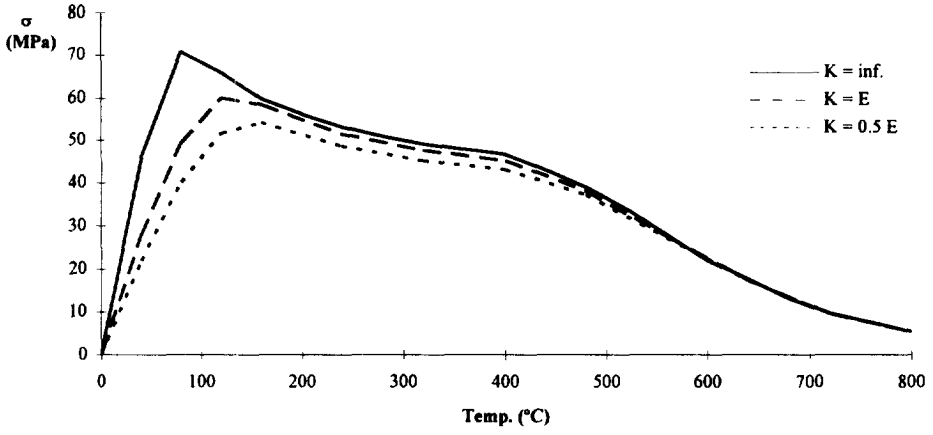

Fig. 18. Comparison of the stress–temperature curves of square plates with different rigidity at the edges and $b/t = 100$, for mild steel.

'ultimate' strength of the plate, i.e. the maximum of the stress–temperature curve, decreases with a reduction in stiffness of the elastic supports.

ACKNOWLEDGEMENTS

This study has been performed within the project 'Optimised Fire Safety of Offshore Structures (OFSOS)' which has been partially funded by the European Commission under the BRITE/EURAM Program, under Contract No. 92/0598. The other partners of this project were Registro Italiano Navale, AEA Petroleum Service, Computational Safety and Reliability, Germanischer Lloyd, SNAMPROGETTI, TECNOMARE, and WS Atkins, having as sponsors AGIP, British Gas, Chevron and Amoco.

REFERENCES

1. Frieze, P. A., Dowling, P. J. and Hobbs, R. H., Ultimate load behaviour of plates in compression. In *Steel Plated Structures*, eds P. J. Dowling *et al.* Crosby Lockwood Staples, London, 1977, pp. 24–50.
2. Harding, J. E., Hobbs, R. H. and Neal, B. G., The elasto-plastic analysis of imperfect square plates under in-plane loading. *Proc. Inst. Civil Engineers*, 1977, **63**(2), 137–158.
3. Little, G. H., The collapse of rectangular steel plates under uniaxial compression. *The Structural Engineer*, 1980, **58B**, 45–60.
4. Crisfield, M. A., Full-range analysis of steel plates and stiffened plating under uniaxial compression. *Proc. Inst. Civil Engineers*, 1975, **59**(2), 595–624.
5. Dow, R. S. and Smith, C. S., Effects of localised imperfections on the compress-

ive strength of long rectangular plates. *J. Constructional Steel Research*, 1983, **3**, 51–76.
6. Ueda, Y. and Yao, T., The influence of complex initial deflection modes on the behaviour and ultimate strength of rectangular plates in compression. *J. Constructional Steel Research*, 1985, **5**, 265–302.
7. Guedes Soares, C. and Gordo, J. M., Compressive strength of rectangular plates under biaxial load and lateral pressure. *Thin Walled Structures*, 1995, **22**, 231–259.
8. Janss, J. and Minne, R., Buckling of steel columns in fire conditions. *Fire Safety J.*, 1981/82, **4**, 227–235.
9. Witteveen, J. and Twilt, L., Behaviour of steel columns under fire action. In *Int. Conf on Column Strength, Proc. IABSE*, Vol. 23, Paris, 1975.
10. Stanzak, W. W. and Lie, T. T., Fire resistance of unprotected steel columns. *J. Struct. Division ASCE*, 1973, **99**, 837–852.
11. Saab, H. A. and Nethercot, D. A., Modelling steel frame behaviour under fire conditions. *Engineering Structures*, 1991, **13**, 371–382.
12. Najjar, S. R. and Burgess, I. W., A non-linear analysis for three-dimensional steel frames in fire conditions. *Engineering Structures*, 1996, **18**(1), 77–89.
13. Guedes Soares, C., Mechanical properties of steels at elevated temperatures. OFSOS Report TEC-C021-02, 1993.
14. Commission For The European Communities, Eurocode No. 3 (EC3): Design of Steel Structures, Part 10: Structural Fire Design, Draft, 1990.
15. Guedes Soares, C., Design equation for the compressive strength of unstiffened plate elements with initial imperfections. *J. Constructional Steel Research*, 1988, **9**, 287–310.
16. Anderberg, Y., Behaviour of steel at high temperatures. RILEM Committee, 44-PHT, 1983.
17. Kirby, B. R. and Preston, R. R., High temperature properties of hot rolled steels for use in fire engineering design studies. *Fire Safety J.*, 1988, **13**, 27–37.
18. Twilt, L., Stress–strain relations of structural steel at elevated temperatures: Analysis of various options and European Proposal. TNO Report BI-91-015, January 1991.
19. ASAS NL, Version 19, WS Atkins Engineering Sciences, UK, 1990.
20. Gordo, J. M. and Guedes Soares, C., Approximate load shortening curves for stiffened plates under uniaxial compression. In *Integrity of Offshore Structures 5*, EMAS, 1993, pp. 189–211.